

# An Elementary Pbs/Mos2 Nanocomposite Photocatalyst for effective visible light Photocatalysis

Badole Sarita Madhukar<sup>1\*</sup>, Dr. Anil Sharma<sup>2</sup>

<sup>1</sup> PhD Student, Kalinga University, Raipur (CG)

<sup>2</sup> PhD Guide, Dept. of Chemistry, Kalinga University, Raipur (CG)

Email - isobesin@gmail.com

**Abstract** - This study investigates nanocomposites for visible-light photocatalytic destruction of organic pollutants, considering the limitations of UV-only photocatalysts. Researchers are currently concentrating on creating, characterising, and evaluating nanocomposite materials that may degrade organic contaminants by visible-light photocatalysis. Nanocomposites are all the rage in the world of photocatalysis due to their large surface area, improved charge carrier separation efficiency, and greater light absorption. The precipitation-deposition method can be used to synthesise PbS/MoS<sub>2</sub> nanocomposite in molar ratios of 0.5, 1, and 1.5 percent. The resulting material can then be characterised using a number of instrumental techniques. By watching how the methylene blue dye degrades, we can track the photocatalytic activity. We will study how pH & catalyst dosage, among other operational parameters, impact photocatalytic activity.

**Keywords** - Nanocomposites, Catalyst, Synthesise PbS/MoS<sub>2</sub>, Photocatalytic

-----X-----

## 1. INTRODUCTION

In recent years, photocatalysis has emerged as a promising technology for addressing environmental pollution and sustainable energy production. Among various photocatalytic materials, semiconductor-based nanocomposites have attracted considerable attention due to their ability to harness solar energy and drive chemical reactions under ambient conditions. In particular, the combination of different semiconductor components in nanocomposites offers synergistic effects that can significantly enhance photocatalytic performance. In this context, the development of nanocomposite photocatalysts has gained momentum, aiming to overcome the limitations of traditional photocatalytic materials, such as narrow light absorption range and low quantum efficiency. One such promising nanocomposite system is composed of lead sulfide (PbS) and molybdenum disulfide (MoS<sub>2</sub>), abbreviated as PbS/MoS<sub>2</sub>, which has shown great potential for effective visible light photocatalysis. Lead sulfide (PbS) is a well-known semiconductor material with a narrow bandgap, enabling it to absorb visible light efficiently. On the other hand, molybdenum disulfide (MoS<sub>2</sub>) possesses unique electronic and optical properties, making it an attractive candidate for photocatalytic applications. By combining PbS with MoS<sub>2</sub> in a nanocomposite structure, it is possible to capitalize on the complementary properties of these

two materials, leading to improved photocatalytic activity under visible light irradiation.

## 2. EXPERIMENTAL

### 2.2.1 Nanoparticles Synthesize of PbS

Pb(NO<sub>3</sub>)<sub>2</sub> & Na<sub>2</sub>S was prepared by dissolving the appropriate amounts in 100 ml of distilled water & stirring the mixture for 30 minutes until it became transparent. The pH was kept at 9 after adding 0.2 molar of NaOH solution to this transparent mixture. For two hours, the reaction mixture mentioned before was vigorously mixed. After filtering the solution, the nanocrystalline lead sulfide was dried in a heating oven set at 110°C. A second round of calcination at 400°C for 2 hours was performed on the lead sulfide nanocrystal.

### 2.2.2 Synthesis of MoS<sub>2</sub> nanoparticles

Typically, 60 mL of distilled water was used to dissolve 2mmol of ammonium molybdate & 10mmol of thiourea in a continuous stirring bath throughout the manufacture of MoS<sub>2</sub> nanoparticles. What next was transferring the mixture to an 80 ml stainless steel autoclave lined with Teflon, sealing it, and then placing it in a preheated oven at 200°C for 24

hours. After that, it was allowed to cool down to room temperature naturally.

### 2.2.3 PbS /MoS2 Nanocomposites Synthesis

The following ingredients were mixed in 200 milliliters of distilled water: 0.2345M ammonium molybdate, 0.5% PbNO<sub>3</sub>, & four hours of stirring to produce a nanocomposite with a PbS-MoS<sub>2</sub> content of 0.5%. After that, the aforementioned solution was mixed with 0.5 M thiourea while being vigorously stirred for three hours. After filtration, the precipitate was rinsed with ethanol & deionized water. According to Y. Li and H. Wang (2011), the last product was then dry for 24 hours at 80° C. The identical method was also used to create nanocomposites with different molar ratios, such as 1% PbS-MoS<sub>2</sub> & 1.5% PbS-MoS<sub>2</sub>.

### 2.2.4 Evaluation of photocatalytic activity

Once photodegradation was finished, the dichromate oxidation method was used to conduct research on chemical oxygen demand (COD). R.Y. Hong's 2009 book details the experimental process for determining COD.

## 3. RESULTS

### 3.1. Characterization

#### UV-vis-DRS

Based on the transformation of their respective diffuse reflectance spectra, the absorption edges of nanocomposites containing 0.5%, 1%, & 1.5% PbS-MoS<sub>2</sub> show a small red shift relative to those of pure PbS & MoS<sub>2</sub>. Applying the formula, we were able to determine the absorption edges and immediately noticeably comparable UV-vis absorption curves.

$$\alpha h\nu = A (h\nu - E_g)^{n/2}$$

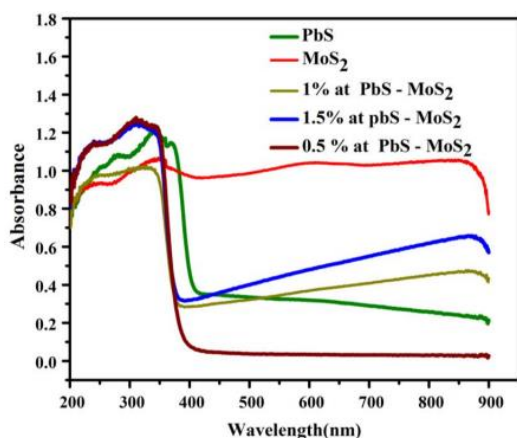


Figure 1: Representation of 0.5%, 1%, 1.5% PbS-MoS<sub>2</sub>

Utilizing the atomic Mulliken electronegativity definition, the position of the band edges of synthetic photocatalysts has been projected analytically.

$$E_{VB} = X - E_e + 1/2E_g$$

$$E_{CB} = E_{VB} - E_g$$

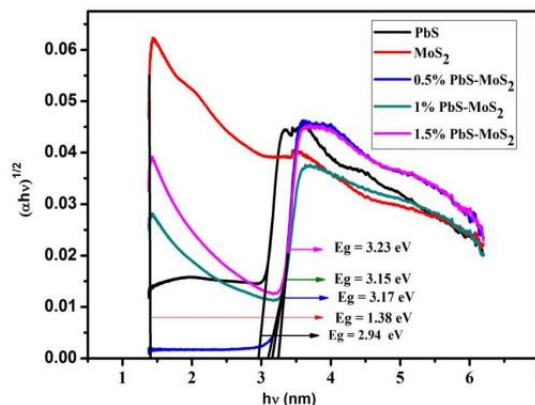


Figure 2:  $(\alpha E \text{ photon})^{1/2}$  Vs  $E \text{ photon}$  curve, At 0.5%, 1% & 1.5% PbS-MoS<sub>2</sub>

Table 1 Evaluated  $E_g$  & determine PbS, MoS<sub>2</sub>  $E_{VB}$  &  $E_{CB}$

Catalyst	X(eV)	$E_{VB}$ (eV)	$E_{CB}$ (eV)	$E_g$ (eV)
PbS	4.92	1.89	-1.05	2.94
MoS <sub>2</sub>	12.28	8.47	7.09	1.38

#### FT-IR Spectrum

Fig.3 displays the Fourier transform infrared spectra of isolated with PbS/MoS<sub>2</sub>. The peaks at 616cm<sup>-1</sup>, 1092cm<sup>-1</sup>, and 1399cm<sup>-1</sup> validate the frequencies attributed to the hetero polar diatomic molecules of PbS (S. Sangeetha 2014). The -OH stretching vibration of water molecules adsorbed on the PbS is responsible for the peak at 3225cm<sup>-1</sup>. A vibrational band at around 600cm<sup>-1</sup> is attributed to Mo-S. It is believed that the MoS<sub>2</sub> absorbed water molecules' H-O-H band is responsible for the wide absorption peaks at 1610cm<sup>-1</sup> & 1396cm<sup>-1</sup>. By combining the absorption peaks of PbS at 665cm<sup>-1</sup> & MoS<sub>2</sub> at 883cm<sup>-1</sup>, the nanocomposite achieves its broad absorption peak. According to K.J. Huang (2014) & D. Zhang (2014), these can be explained by the way PbS & MoS<sub>2</sub> interact in the nanocomposite.

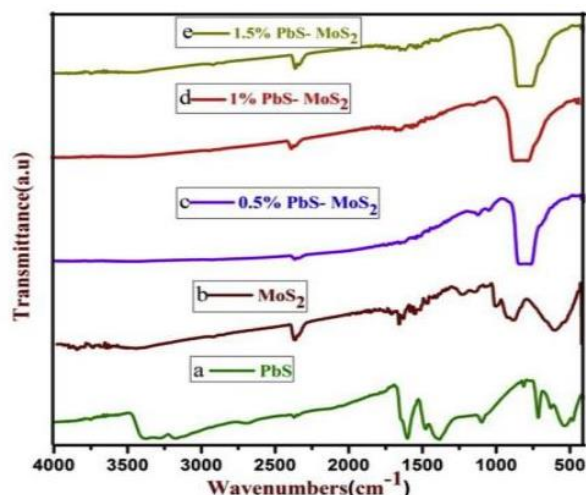


Figure 3: FT-IR spectra

### Photoluminescence (PL) Spectra

The material's photoluminescence (PL) spectra can reveal the photo-induced electron & hole separation and recombination processes (J.Di, J.X.Xia 2014;). With less electron-hole recombination and hence more photocatalytic activity, the PL intensity is low. Figure 4 displays the PL spectra of PbS, MoS<sub>2</sub>, & 1% PbS-MoS<sub>2</sub> at ambient temperature. Here is the sequence in which the prepared samples' PL intensities decreased: A concentration of PbS greater than MoS<sub>2</sub> is greater than 1% PbS/MoS<sub>2</sub>.

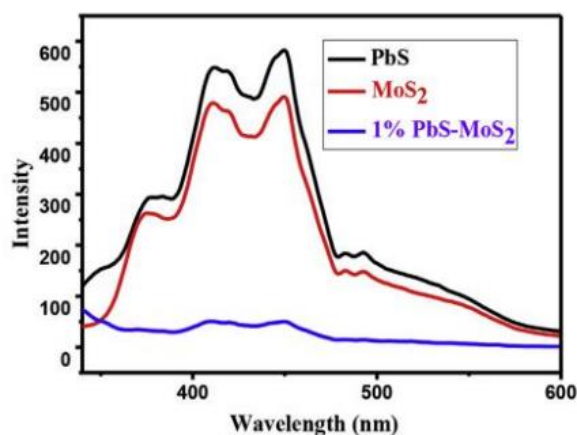


Figure 4: PL spectra of PbS, MoS<sub>2</sub> & 1% PbS-MoS<sub>2</sub>

### X-ray diffraction

Crystal structure analysis using XRD was performed on the PbS, MoS<sub>2</sub>, & PbS-MoS<sub>2</sub> nanocomposites. Figure 5 displays the XRD designs of the samples that were prepared. The majority of the diffraction peaks in the pure PbS sample can be observed at 2θ angles of 26.2°, 33.2°, 39.4°, and 44.3°, which correspond to the indices of the (1 1 1), (0 0 2), (2 2 0), and (2 2 0) lattice planes, correspondingly.

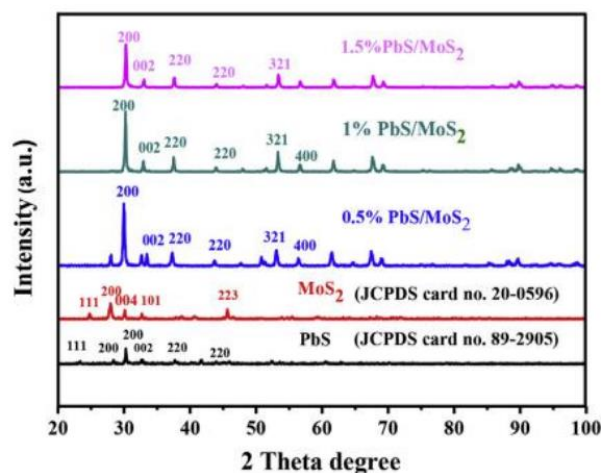


Figure 5: XRD pattern of PbS, MoS<sub>2</sub>, At 0.5%, 1% & 1.5% PbS-MoS<sub>2</sub>

### 3.2 Photodegradation of MB

At a pH of 11.5 (Fig. 6), the degradation of MB was evaluated to investigate the photocatalytic activity of PbS, MoS<sub>2</sub>, & PbS-MoS<sub>2</sub> nanocomposite. After thirty minutes of visible light deterioration of the MB, photocatalysts were not used. The control investigations showed that the produced photocatalysts absorbed dye at their active sites when left in darkness for half an hour with photocatalytic materials. A photocatalytic degradation efficacy of 83% at 800 nm was achieved in an aqueous solution having 1% PbS-MoS<sub>2</sub> following 180 minutes of UV irradiation. The degrading efficiency of the photocatalyst is as follows: PbS > MoS<sub>2</sub> & findings given, for concentrations of PbS-MoS<sub>2</sub> ranging from 1% to 1.5% to 0.5%. The photocatalytic action to the breakdown of MB is best exhibited by the 1%PbS-MoS<sub>2</sub> heterojunction, as compared to bare PbS and MoS<sub>2</sub>.

Table 2: Constraints derived by observations of N<sub>2</sub> adsorption-desorption

Sample	Specific surface area (m <sup>2</sup> /g)	Average pore diameter (nm)	Pore volume (cm <sup>3</sup> /g)
PbS	37.34	28.09	0.2654
MoS <sub>2</sub>	35.49	42.82	0.3041
0.5% PbS-MoS <sub>2</sub>	56.65	39.96	1.2325
1% PbS-MoS <sub>2</sub>	60.74	96.88	0.7485
1.5% PbS-MoS <sub>2</sub>	45.12	42.79	0.1410



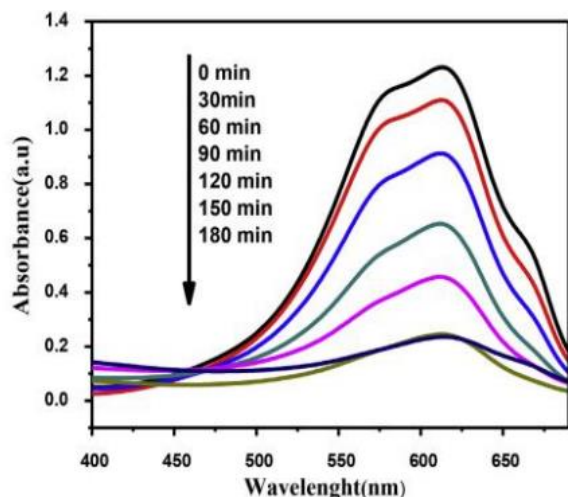


Figure 6: Time dependent UV-vis spectral changes of methylene blue (0.03M) in Presence of PbS-MoS<sub>2</sub> (1%) (0.4g/L)

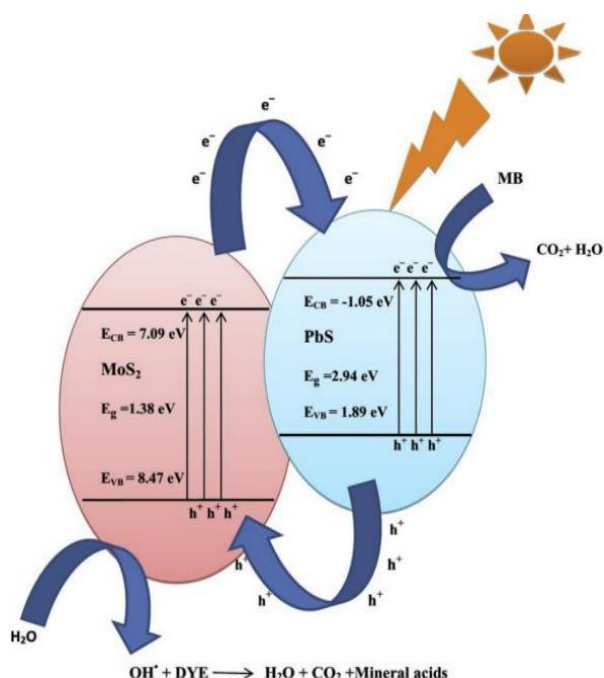


Figure 7: The electron transfer schematics in 1% PbS/MoS<sub>2</sub> when tested with UV irradiation

### 3.3 Optimization of reaction parameters

#### Effect of pH

Figure 8 displays the findings of an experiment that tested the impact of pH on photodegradation efficiency over a pH range of 3 to 11.5 using a constant MB concentration of 0.3mM, a catalyst dosage of 0.4 g/L, & irradiation period of 180 minutes. At pH 11.5 we have the highest degradation efficiency of 83%. The MB chromophore has a positive electrical configuration, which is why basic dyes are also known as cationic dyes. The negatively charged photocatalyst is produced at high pH, which improves the catalyst's electron transfer rate & available active surface area. Electrostatic attraction makes quick work of adsorbed

photocatalyst onto positively charged MB. The photocatalyst's surface also makes it easier to generate more superoxide & hydroxyl radicals at high pH. (M.M. Uddin 2007; Q.J. Xiang 2011)

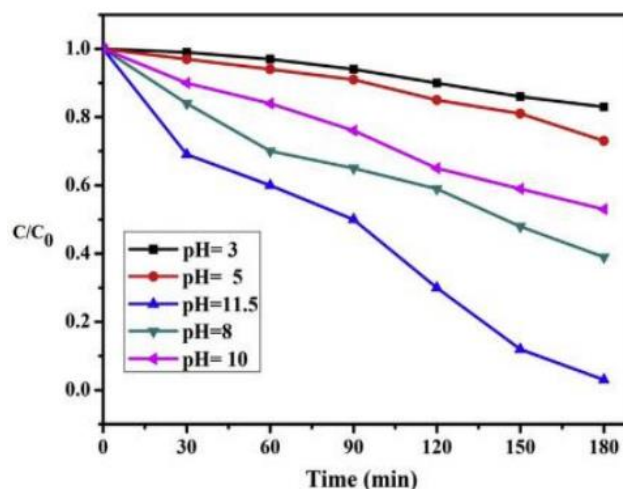


Figure 8: pH effect of MB Photodegradation

#### Effect of Catalyst Dosage

An important factor influencing the rate of organic molecule degradation in photocatalytic reactions is the concentration of photocatalyst. To investigate the effect on the photodegradation rate of MB, the concentration of 1% PbS-MoS<sub>2</sub> was adjusted from 0.4g/L to 0.9 g/L. Results under UV irradiation for 5 hours were obviously insignificant when comparing results with and without 1% PbS-MoS<sub>2</sub> photocatalysts at different dosages (Fig.9). Although the photocatalytic degradation rate was linearly proportional to the dosage of 1% PbS-MoS<sub>2</sub>, it was slowed down at extremely high dosages. Since the overall surface area or the number of available active sites for the photocatalytic process grew with increasing dosages of 1% PbS-MoS<sub>2</sub>, it is likely that the rate improved as well. Overdosing on 1% PbS-MoS<sub>2</sub> reduced the incoming visible light intensity owing to increased light scattering or reduced light penetration, negating the beneficial effect of the dosage rise. As a result, the photocatalyst could absorb less light or activate fewer catalyst sites. Because the nanocomposites clumped together when the photocatalyst dosage was high, the surface area was also reduced. (J. Yu 2007; H.F. Lai 2014)

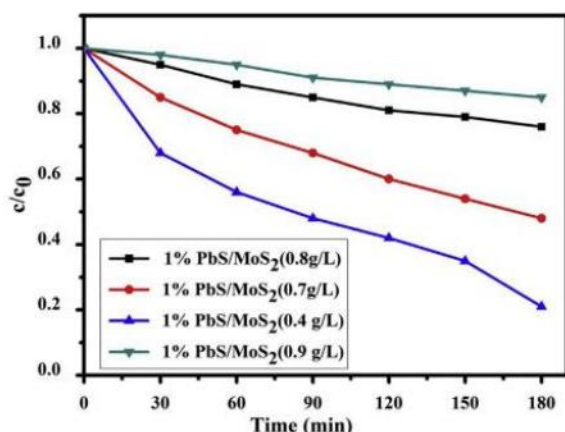


Figure 9: Catalyst dosage Effect of MB photodegradation

#### Photodegradation MB: Kinetics analysis

We examined the visible-light MB kinetics of all photocatalysts utilizing the pseudo-first-order equation (W. Zhao, 2010).

$$-\ln(C_0/C) = kt$$

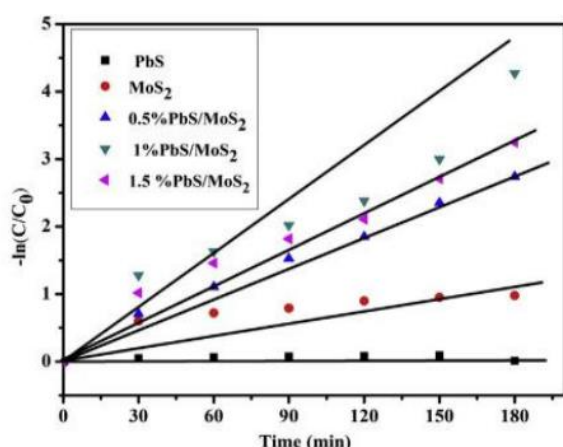


Figure 10: Photocatalytic degradation of MB under a kinetic regime

Table 3: Pseudo first rate constant values photocatalysts

Time (min)	Rate Constant K (min <sup>-1</sup> )				
	PbS (10 <sup>-3</sup> S <sup>-1</sup> )	MoS <sub>2</sub> (10 <sup>-3</sup> S <sup>-1</sup> )	0.5% PbS / MoS <sub>2</sub> (10 <sup>-3</sup> S <sup>-1</sup> )	1%PbS / MoS <sub>2</sub> (10 <sup>-3</sup> S <sup>-1</sup> )	1.5% PbS / MoS <sub>2</sub> (10 <sup>-3</sup> S <sup>-1</sup> )
30	0.053	0.60	0.71	1.28	1.02
60	0.065	0.72	1.11	1.63	1.46
90	0.076	0.79	1.53	2.02	1.82
120	0.083	0.90	1.85	2.38	2.11
150	0.092	0.95	2.35	3.00	2.71
180	0.010	0.98	2.74	4.27	3.25

#### COD

As a proxy for the organic matter's oxygen equivalent, the COD was applied to samples that could be oxidized to CO<sub>2</sub> & water by a potent oxidant. The conditions under which the photocatalytic studies were conducted

were perfect. Throughout the procedure, test samples were taken at 30-minute intervals. The estimated COD of the MB both before & after visible light irradiation is displayed in Table 4. After 180 minutes of photodegradation under ideal conditions, the COD of the resulting solutions dropped to 83.000%. The results showed that the chemical oxygen requirement drops because most organic materials in MB breaks down into smaller species, particularly inorganic compounds.

Table 4: Level of COD removed from MB (in milligrams per liter) by photodegradation with 1% PbS/MoS2 exposed to visible light

Time (Min)	COD removal efficiency (%) Methylene blue
0	0
30	8.53
60	20.32
90	34.24
120	48.24
150	64.54
180	83

#### 4. CONCLUSIONS

Using a precipitation-deposition technique, we were able to successfully create nanocomposite with varying molar ratios, and we have documented its structural and optical characteristics. The as-prepared catalysts, which are made of PbS with a tetragonal structure and MoS<sub>2</sub> with a hexagonal structure, are reflected in the XRD patterns. SEM analysis shows that PbS-MoS<sub>2</sub> has grown into a sheet-like structure. The EDX study proved that the only elements included in the manufactured PbS-MoS<sub>2</sub> nanocomposites are lead, molybdenum, and sulfur. A meso-porous structure was deduced from the generated hetero-junctions using BET-surface area analysis. The visible-light absorption edge of PbS-MoS<sub>2</sub> nanocomposites is shown by DRS analysis. Solution pH and catalyst dosage are clearly impacted by photodegradation of MB, according to the data. There is additional speculation about a photocatalytic mechanism. At 180 minutes with a pH of 11.5 and a dosage of 0.4g/L of 1% PbS-MoS<sub>2</sub> and a concentration of 0.3Mm of MB, the reaction conditions are maximized, as maximal photodegradation is attained. On the produced catalysts, the photodegradation of MB follows a pseudo-first-order model. In terms of photocatalytic activity towards MB degradation, characterization suggests that 1% PbS-MoS<sub>2</sub> exhibited the highest results due to its relatively greater specific surface area & effective electron hole separation. This study's findings corroborate previous research showing that PbS-MoS<sub>2</sub> is a potential photocatalyst for organic dye degradation in water.

## REFERENCES

1. Anjum, M., Kumar, R., & Barakat, M. A. (2017). Visible light driven photocatalytic degradation of organic pollutants in wastewater and real sludge using ZnO–ZnS/Ag<sub>2</sub>O–Ag<sub>2</sub>S nanocomposite. *Journal of the Taiwan Institute of Chemical Engineers*, 77, 227–235.
2. Anwer, H., & Park, J. W. (2018). Synthesis and characterization of a heterojunction rGO/ZrO<sub>2</sub>/Ag<sub>3</sub>PO<sub>4</sub> nanocomposite for degradation of organic contaminants. *Journal of hazardous materials*, 358, 416–426.
3. Babu, P Reddy, MV Revathi, N & Reddy, KTR 2011, 'Effect of pH on the physical properties of ZnIn<sub>2</sub>Se<sub>4</sub> thin films grown by chemical bath deposition', *Journal of Nano- Electronic Physics*, vol. 3, no. 1, pp. 85–91.
4. Bifen Gao, AshokChakraborty, Ji-minYang and Wan in lee 2010, 'Visiblelight photocatalytic activity of BiOCl/Bi<sub>2</sub>SO<sub>4</sub> nanocomposites', *BulletinKorean Chemical Society*, Vol. 31(7), pp.1941–1944.
5. C. Y. Xu, Photoactivity and stability of Ag<sub>2</sub>WO<sub>4</sub> for organic degradation in aqueous suspensions, *Applied Surface Science*, 319, (2014) 319–323.
6. Dai, J. Lv, L. Lu, C. Liang, Lei Geng, G. Zhu, A facile fabrication of plasmonic g-C<sub>3</sub>N<sub>4</sub>/Ag<sub>2</sub>WO<sub>4</sub>/Ag ternary heterojunction visible-light photocatalyst, *Materials Chemistry and Physics*, 177 (2016) 529–537.
7. Ehrampoosh, M, Moussavi, GH, Ghaneian, M, Rahimi, S and Ahmadian, M 2011, 'Removal of methylene blue dye from textile simulated sample using tubular reactor and TiO<sub>2</sub>/UV-C photocatalytic process', *Journal of Environmental Health Science and Engineering*, Vol. 8(1), pp.34–40.
8. Fu, X., Zhang, Y., Cao, P., Ma, H., Liu, P., He, L., ... & Zhai, M. (2016). Radiation synthesis of CdS/reduced graphene oxide nanocomposites for visible-light-driven photocatalytic degradation of organic contaminant. *Radiation Physics and Chemistry*, 123, 79–86.
9. Gondal, MA, Rashid, SG, Mohamed Abdulkader Dastager, Varanasi, KK 2013, 'Sol-Gel synthesis of Au/cu-TiO<sub>2</sub> Nanocomposite and their morphological and optical properties', *IEE Photonics*, Vol.5, No.3
10. Hendia, TA & Soliman, LI 1995, 'Optical absorption behaviour of evaporated ZnIn<sub>2</sub>Se<sub>4</sub> thin films', *Thin Solid Films*, vol. 261, no. 1–2, pp. 322–327. Lin, SH & Lu, CH 2014, 'Solution synthesis and characterization of n-type zinc 129.
11. J. Fowsiya, G. Madhumitha, N. A. Al-Dhabi, M. V. Arasu, Photocatalytic degradation of Congo red using Carissa edulis extract capped zinc oxide nanoparticles, *Journal of Photochemistry & Photobiology, B: Biology* 162 (2016) 395–401.
12. Khataee, AR Hosseini, M Hanifehpour, Y Safarpour, M & Joo, SW 2014, 'Hydrothermal synthesis and characterization of Nd-doped ZnSe nanoparticles with enhanced visible light photocatalytic activity', *Research on Chemical Intermediates*, vol. 40, no. 2, pp. 495–508.
13. Mukhlsh, MB, Najnin, F, Rahman, MM and Uddin, MJ 2013, 'Photocatalytic degradation of different dyes using TiO<sub>2</sub> with high surface area: A kinetic study', *J.Sci.Res.* Vol.5, no.2, pp.301–314.
14. N.A. Abdelwahab, F.M. Helaly, Simulated visible light photocatalytic degradation of Congo red by TiO<sub>2</sub> coated magnetic polyacrylamide grafted carboxymethylated chitosan, *Journal of Industrial and Engineering Chemistry*, 50 (2017) 162–171.
15. Romero-Saez, M, Jaramillo, LY, Saravanan, R, Benito, N, Pabon, E, Mosquera, E, Gracia, F 2017, 'Notable Photocatalytic activity of TiO<sub>2</sub>-Polyethylene nano composites for visible light degradation of Organic Pollutants', *express polymer letter*, Vol. 11, No. 11, P.No.899–909.
16. S. Sivasankaran, "Composite Materials, Nanocomposites, Recent Evolutions", 2019, DOI: 10.5772/intechopen.73364, ISBN:978-1-78985-012-3, Intech Open Publications.
17. T. Yao, W. Jia, Y. Feng, J. Zhang, Y. Lian, J. Wu, X. Zhang, Preparation of reduced graphene oxide nanosheet/FexOy/nitrogen-doped carbon layer aerogel as photo-Fenton catalyst with enhanced degradation activity and reusability, *Journal of Hazardous Materials*, 362 (2019) 62–71.

## Corresponding Author

Badole Sarita Madhukar\*

PhD Student, Kalinga University, Raipur (CG)